Spatial Coherence of Impact Pressures at a Vertical Breakwater in Multidirectional Seas

Sauer, W.; Löffler, A.; Kortenhaus, A.; Archetti, R.; Burcharth, Hans Falk; Frigaard, Peter Bak; Koether, G.; Lamberti, A.; Martinelli, L.

Publication date:
1999

Document Version
Publisher's PDF, also known as Version of record

European Commission
Training and Mobility of Researchers Programme
Access to Large-scale Facilities
IAS 0154/ 96 E

Spatial coherence of impact pressures at a vertical breakwater in multidirectional seas
-Set-up of the experiment and report on the activities-

prepared by
Wiebke Sauer, Annika Löffler, Andreas Kortenhaus,
Renata Archetti, Hans F. Burcharth, Peter Frigaard, Gunnar Koether,
Alberto Lamberti, Luca Martinelli

March 1999

UK Coastal Research Facility at HR Wallingford
October 1998 - January 1999

University of Bologna
DISTART Idraulica

Technical University of Braunschweig
Leichtweiss-Institut

Aalborg University
Hydraulics and Coastal Engineering Laboratory

Contents

Annex A

Annex B

Annex C

Annex D

Annex E

Annex F

List of Figures

List of tables

List of symbols

B_c	[m]	Width of caisson
D_{50}	[mm]	Diameter of stone which exceeds the 50% value of sieve curve (mean particle size)
d	[m]	Water depth over berm in front of wall
f	[Hz]	Wave frequency
f_p	[Hz]	Frequency of peak of wave energy spectrum
$G(\theta)$	[-]	Spreading function
g	[m/s²]	Gravitational acceleration
H_S	[m]	Significant wave height
H_{0S}	[m]	Significant wave height in deep water
h_0	[m]	Water depth in deep water
h_b	[m]	Height of berm above sea bed
h_c	[m]	Height of caisson
h_s	[m]	Water depth at toe of structure/mound
L_0	[m]	Deep water wave length
L_p	[m]	Deep water wave length related to peak period
S(f)	[m²·s]	Spectral density
$S(f,\theta)$	[m²·s]	Directional spectral density
s_p	[-]	Deep water wave steepness
T_p	[s]	Wave period of spectral peak
T_{0p}	[s]	Wave period of spectral peak in deep water
γ	[-]	Peak factor of JONSWAP spectrum
θ	[°]	Direction of wave propagation
θ_0	[°]	Mean wave direction

Keywords
Vertical Breakwater, Impact Pressures, Uplift, Three-dimensional Model Tests

1. Introduction

The programme "Training and Mobility of Researchers" (TMR) within the 4th Framework Programme of the European Commission is divided into three independent activities: research networks, access to large-scale facilities and training through research. The activity 2 "Access to Large-scale Facilities" (LSF) includes the possiblity for researchers to work at selected European large-scale facilities. Within this activity the project "Spatial coherence of impact pressures at a vertical breakwater in multidirectional seas" was founded and could therefore be performed by the University of Bologna (DISTART Idraulica, Italy [UoB]), Aalborg University (Hydraulics and Coastal Engineering Laboratory, Denmark [AU]) and Technical University of Braunschweig (Leichtweiss-Institut, Germany [LWI]).

In this project a physical model of the Genoa Voltri breakwater (for a description of the breakwater see Martinelli (1998)) was set up at an approximate scale of 1:100 and loaded by short crested waves in the wave basin of the UK Coastal Research Facility (CRF) at HR Wallingford.

The main objective of the project is to provide information about the horizontal coherence of breaking wave pressures and forces at vertical walls.

Observations from three-dimensional model tests have shown, that very high jets indicating very high pressure induced by breaking waves do not extend to a whole caisson length (see Frigaard et al. (1998)). Considering this effect a lower total force to one caisson will be obtained than the one that results from applying the maximum force per unit length to the full length of the caisson.

It is of special interest in the project to investigate how the relative extreme wave forces per unit length due to breaking waves increase with decreasing length of the caisson. This may be achieved by finding the lateral force distribution over a caisson length.

The use of a physical model is necessary because the process of wave breaking is included. Breaking is a highly non-linear process and it is very difficult to give analytic solutions for problems including this process. Also the three-dimensional process of

breaking is too complex and would need too much computation capacity to be described by numerical models.

Further objectives of the experiments are to measure the simultaneous values of horizontal and uplift pressures, from which the resulting forces and moments can be calculated.

This report describes the model set-up of the experiments and the activities performed at HR Wallingford between October 1998 and January 1999. The data analysis and results of the experiments will be described in a technical report which is supposed to be published in autumn 1999.

2. Description of the model set-up

2.1 Bathymetry

The wave basin of the UK Coastal Research Facility is 54 m long and 27 m wide where an area of 36 m × 27 m can be used for testing. Waves with a wave height of up to 20 cm and currents with a maximum speed of 0.14 m/s can be generated.

A new bottom geometry of the basin was provided for the project consisting of

- a 1:20 foreshore slope starting 12.3 m from the back of the basin,
- a 0.20 m high plane area 5.9 m long, and
- an absorbing beach with an 1:6 slope.

There was no variation over the length of the basin (see Figures 1 and 2). Sand and gravel covered by a thin layer of concrete was used for the plane area and the 1: 20 slope, flint stones (D_{50}=40 mm) were used to build the absorbing beach.

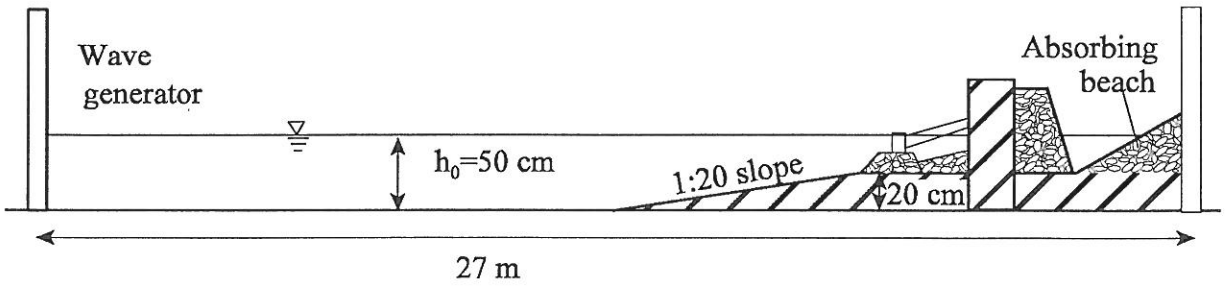

Figure 1: Cross section of the short side of the basin (A-A, section in Figure 2)

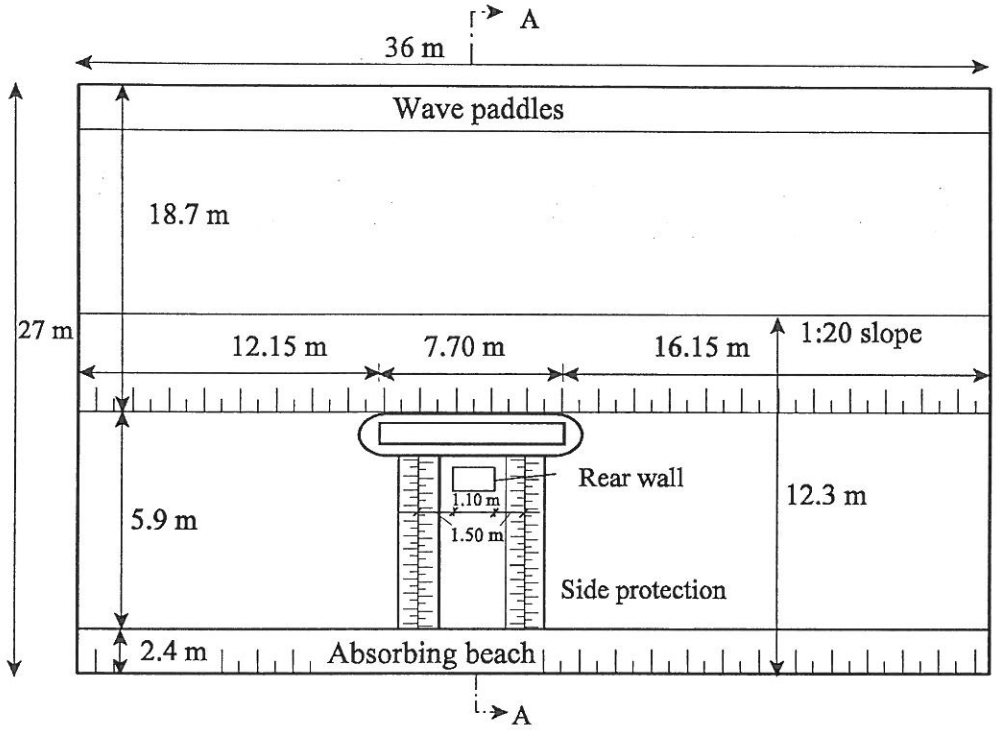

Figure 2: CRF wave basin, plan view

2.2 Breakwater and construction behind the breakwater

The breakwater model was constructed in the 5.9 m long plane area. For avoiding too much effect from diffraction during the tests with oblique wave direction, the model is located 2 m left of the centre of the basin (see Figure 2).

The length of the breakwater was 7.70 m in total, the test section made of seven independent aluminium caissons was 1.10 m long (see Figure 3).

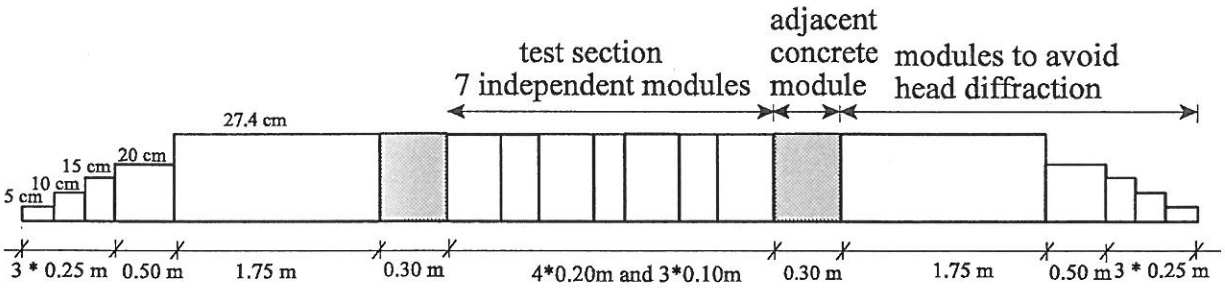

Figure 3: Front view of breakwater

The caisson elements for the test section of the breakwater were made of aluminium. Three of the modules were 0.10 m long, 0.185 m wide and 0.274 m high and four were 0.20 m long, 0.185 m wide and 0.274 m high (see Figures 3 and 4). They had a one mm gap between them assured by small teflon pieces.

The modules were filled with crushed limestone and sand. The larger modules had a dry weight of 16.7 kg in total and the smaller modules of 8.95 kg. Sand was glued on the bottom of the modules to increase the roughness and to obtain a similar behaviour of the aluminium model as compared to the prototype caissons (concrete). Additionally, this should avoid wave induced currents influencing the uplift pressure transducers.

The breakwater was situated on a 0.1 m high rubble mound foundation with berm slopes of 1:2 on each side and a total width of 0.45 m at its crown (see Figure 4). The rubble mound consisted of crushed limestone with a grain size of 5 to 10 mm. However, during the preliminary test phase it has been observed that the rubble mound was significantly damaged by the waves so that a larger grain size was necessary. Hence, crushed limestone with a grain size between 14 to 20 mm replaced the top layer of the rubble mound.

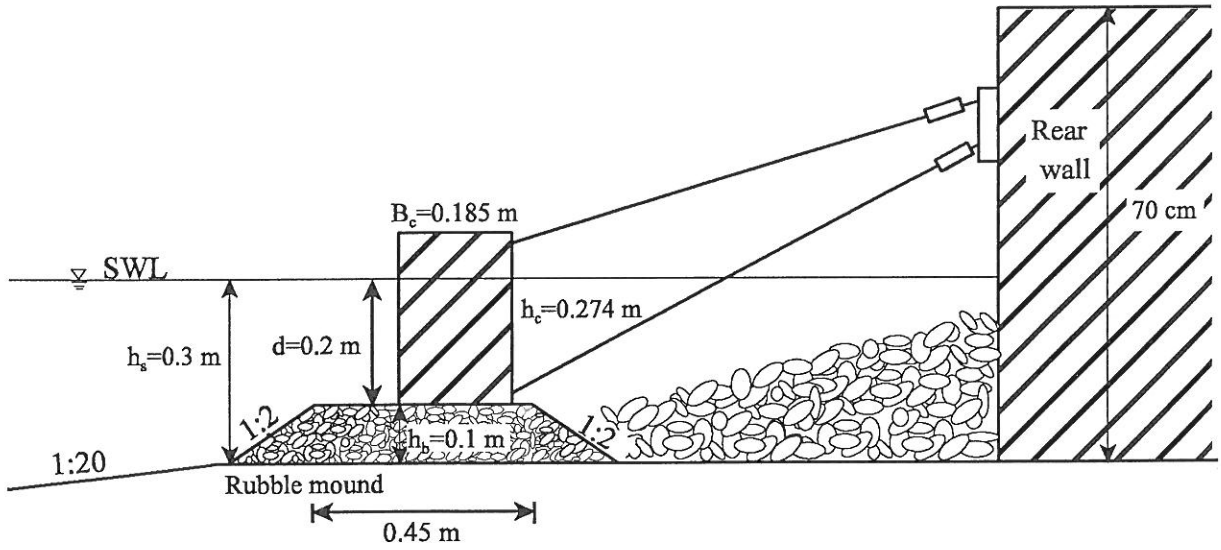

Figure 4: Cross section of breakwater

Aluminium foot protection blocks have been placed in front of the structure (see Figure 5). The foot protection blocks are similar to concrete blocks used as foot protection at the prototype breakwater in Genoa. For a detailed description of the prototype

breakwater see Martinelli (1998).

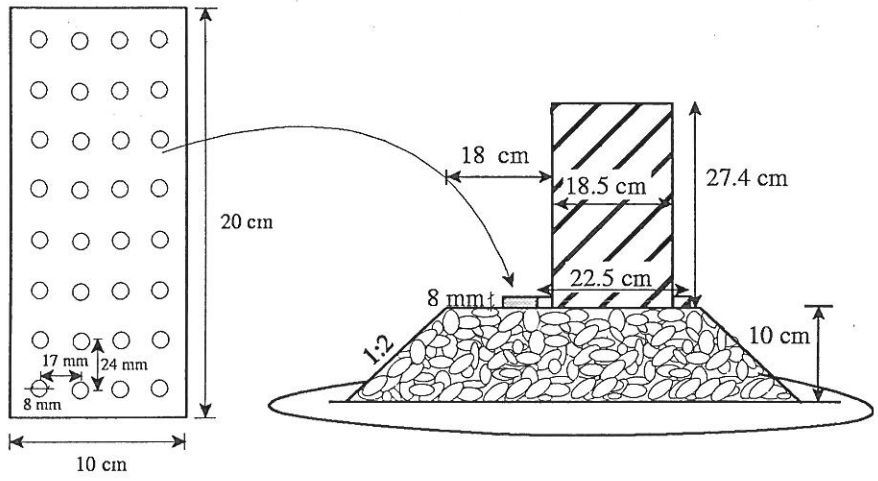

Figure 5: Protection blocks

Two adjacent breakwater modules, 0.30 m long and made of concrete are positioned to check if sliding takes place (Figure 3). Their weight was similar to the prototype caissons. To stabilize the rubble mound behind the concrete modules, they were supported by large concrete bricks and an aluminium frame in test phase A (see Figure 6). In test phase B the displacement of the adjacent concrete modules has been measured by amplifiers which were installed at the rear side of the modules (see Photo 1, Annex D). Additionally, during the last test phase (BB) the bottom of one of the adjacent modules has been made smoother and the bottom of the other one has been made rougher in order to investigate the influence of the roughness of the surface on the sliding.

To ensure that there was no direct contact between the aluminium caissons and the adjacent concrete modules a construction of two aluminium plates with pointed ends that were sunk in the rubble mound, and three aluminium bars were used to "connect" the seven caissons (see Photo 1, Annex D).

Beside the test section (consisting of aluminium modules for measuring forces and pressures and concrete modules for measuring sliding) several 3.0 m long adjacent modules made of concrete varying in height were used to avoid head diffraction (see Figure 3). Additionally, gravel was added at both ends of the breakwater section with the same purpose. This procedure allowed measurements without head diffraction giving results valid for an arbitrary part of the breakwater and not for the special part at the end.

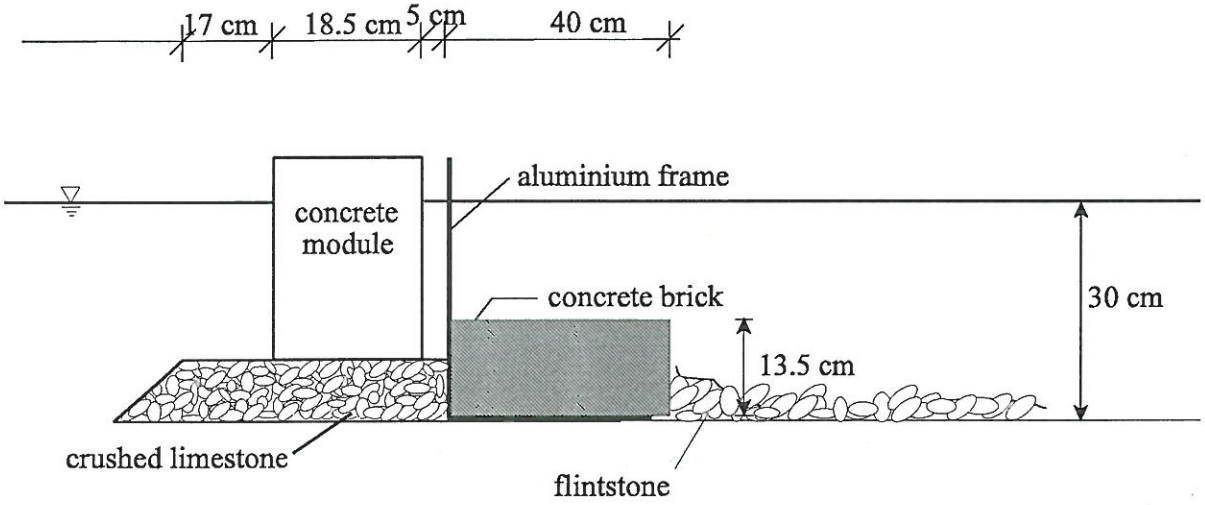

Figure 6: Adjacent concrete module and supporting construction

A rear wall 1.10 m long, 0.665 m wide and 0.70 m high was constructed behind the test section of the breakwater to support the force transducers (see Figure 9). The wall was made of concrete brick walls filled with concrete in the middle.

A side protection consisting of concrete brick walls and surrounded by gravel was built (see Figure 2 and Photo 8, Annex D) to enable measurements of wave transmission and to avoid waves at the rear side of the breakwater. The side protection is about 10 cm higher than the still water level.

2.3 Test configurations

There were two main configurations for the experiment each composed of two test phases and therefore four test phases at all:

a) Test phase AA: pressures at the front of the breakwater and uplift pressures were measured at the centre module with high density (11 pressure transducers, see Figure 7), the total force was measured by two force transducers on four caissons (see Figure 10), the force transducers were concentrated in the centre of the test section to provide data over small distances

b) Test phase AB: as test phase AA, but the force transducers were spread over the whole length of the test section in order to provide data over larger distances (see Figure 10)

c) Test phase BA: forces and uplift pressures were measured, the whole length of the test section was used for measuring forces, the uplift pressure transducers were concentrated in the centre of the test section (data over small distances, see Figure 10)

d) Test phase BB: as test phase BA, but uplift pressure transducers were spread over the whole length of the test section (data over long distances, see Figure 9)

Test phase A was an exploratory and verification test phase since integrated pressures at the front of the caissons were compared to the measured forces and the set-up of the force transducers was checked (see section 2.5, Force transducers).

2.4 Pressure transducers

In test phase AA and AB a special module was used with seven positions of pressure transducers to measure horizontal pressures and four pressure transducers to measure uplift pressures (see Figure 7).

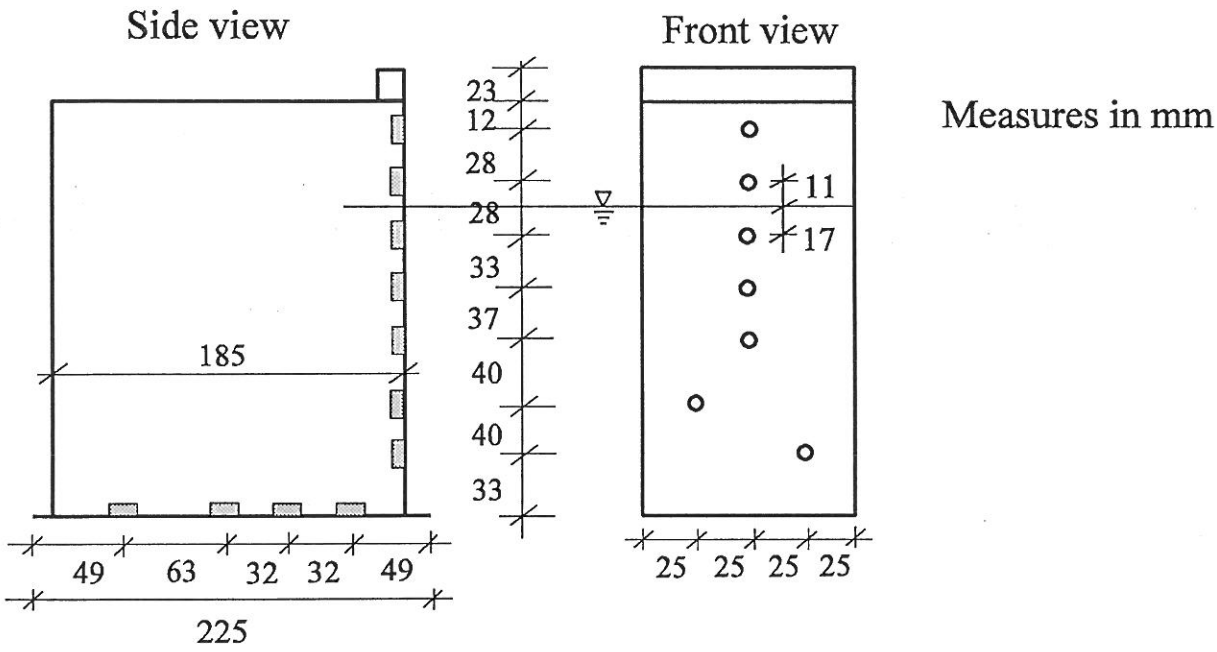

Figure 7: Positition of pressure transducers for configuration AA and AB

The use of the same position of the pressure transducers in test phase AA and AB was also useful to get information about the repeatability of the tests because tests with the same wave parameters as used in test phase AA have been repeated in test phase AB.
In configuration BA and BB the uplift pressure transducers were positioned as shown in Figure 8.
A thin layer of a silicon-like material was used for protection of the pressure transducers against grains of sand and other soil particles. The material was supposed to be incompressible, so that the measurements were not disturbed.
The pressure transducers were from Druck, PCDR 800 Series with a measurement range of up to 10 bar. They have been calibrated by compressed air and recording of the corresponding values in Volt which allowed to give the calibration constants. During the testing further calibrations have been carried out between test phases A and B by measuring hydrostatic pressures at different water levels. The amplification values, calibration constants, maximum pressures and resolutions of the pressure transducers are given in Annex E, respectively.

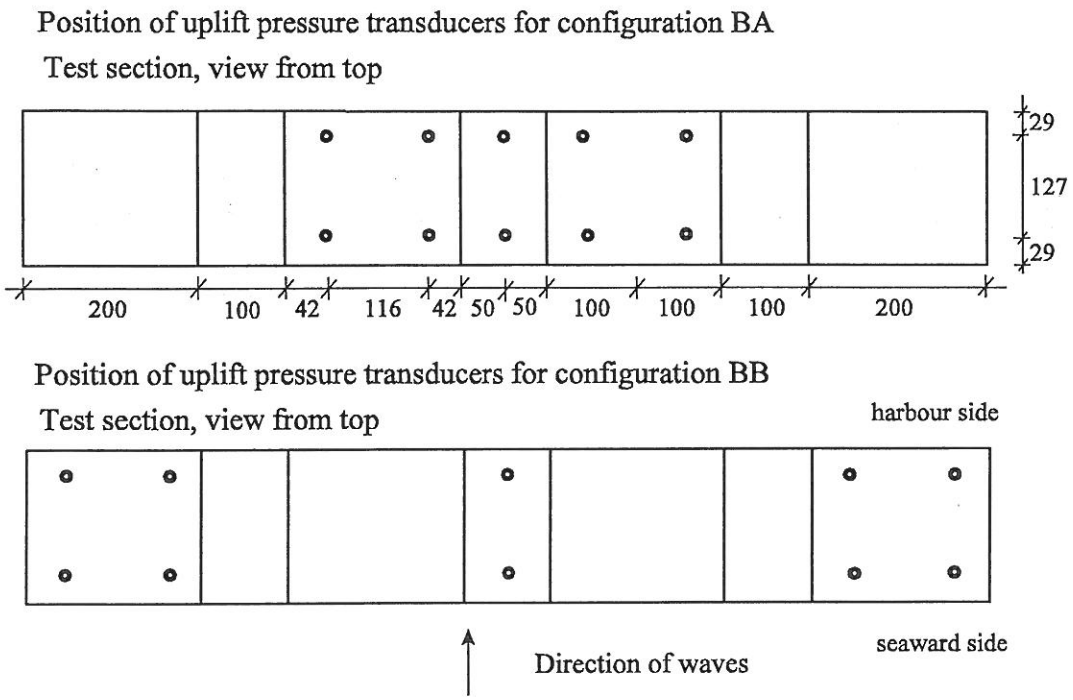

Figure 8: Positions of pressure transducers for configuration BA and BB

2.5 Force transducers

Eight force transducers were used to measure the forces on the breakwater. The force transducers were connected to a massive rear wall in order to avoid any movement. For this construction a steel plate (1.10 m × 0.20 m) was anchored in the concrete rear wall, the force transducers were connected to the steel plate and to a bar (aluminium, diameter 14 mm) on the other side that was connected to the modules at a certain angle. Every breakwater module had a bar close to the top and the bottom allowing the connection of a force transducer (see Figure 9 and Photo3, Annex D).

The lateral position of the force transducers for the different configurations is shown in Fig.10.

The force transducers were of type U-400 from Maywood Instruments Limited. Four of the eight force transducers had a maximum load of 100 kg, the other four had a maximum load of 50 kg. For calibration, different weights were applied to the force

transducers. All forces were amplified by a factor of 500 and low-pass filtered at 100 Hz. The amplification values, calibration constants, maximum pressures and resolutions of the force transducers are given in Annex E, respectively.

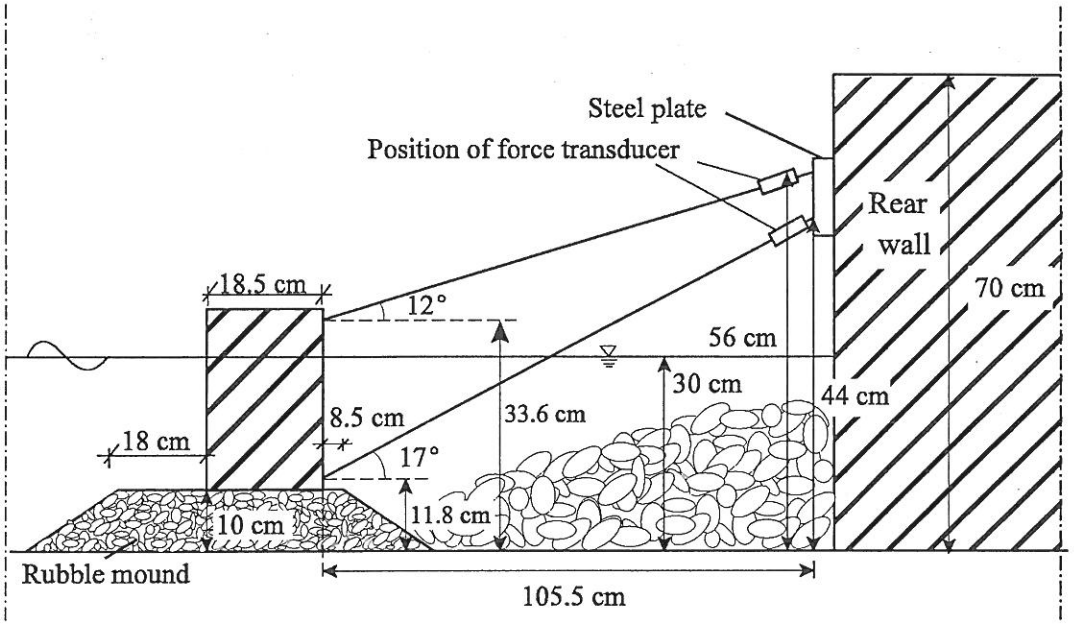

Figure 9: Positions of force transducers at the breakwater model

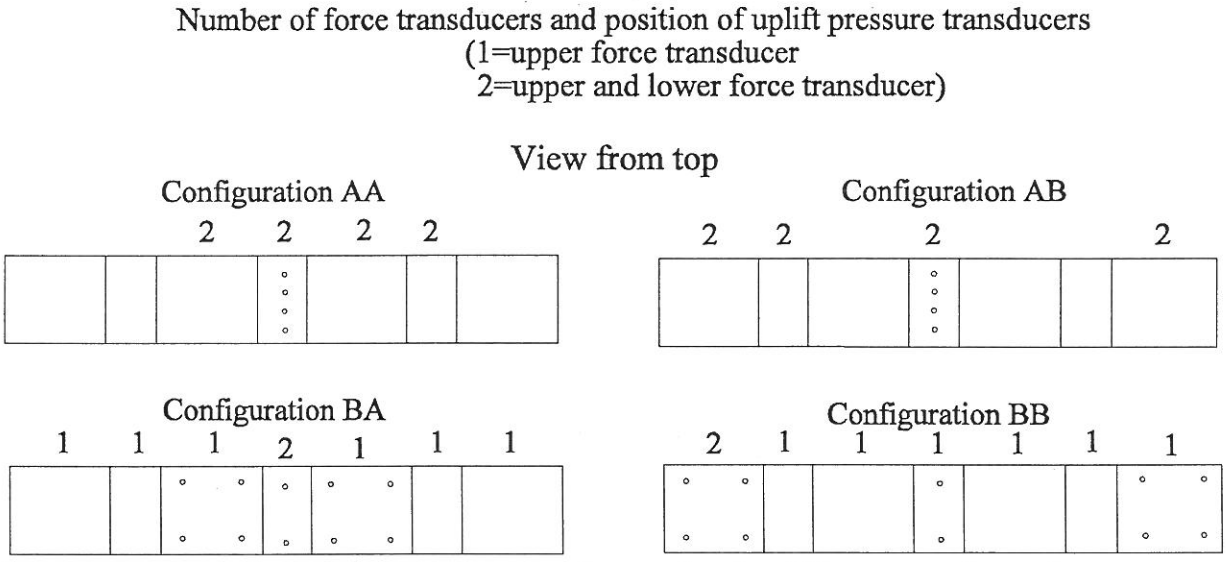

Figure 10: Lateral position of force transducers for the different configurations

The force transducers were fixed to the caissons with angles of 12° (upper force transducer) and 17° (lower force transducer). This was thought to be useful as the intersection of the line of effect of the force measured by the upper force transducer and

the line of effect of the total wave induced horizontal force is at the application point of the total horizontal force close to the SWL. Therefore, most of the wave induced forces were directly transfered to the upper force transducer. The lines of effect of the two force transducers also intersect due to their angles which allowed for easier calculation of the unknown reactions of the rubble mound.

A further reason for the inclined position of the force transducers was to protect them against water splashes although they were made waterproof.

In test phase AA and AB upper and lower force transducers were positioned on four caisson modules. By measuring the forces and moments by two different force transducers the stiffness and the response of the rubble mound were understood. If these phenomena were known it was principally possible to just use the upper force transducer at each caisson for the assessment of the total horizontal force induced by the waves during test phase B. In configuration BA and BB the force transducers were only positioned in the upper part and only the eighth one was positioned in the lower part. The lower bars were only used for stabilization in test phase B.

The relationship between forces in the upper and lower force transducer and the response of the underlying rubble mound foundation were also investigated in the preliminary dry tests results of which will be described in the technical report.

2.5 Wave gauges

An array of seven wave gauges was placed at the toe of the 1:20 slope in order to analyse the incident wave field (in test phase A only five wave gauges from this array were used, in test phase B all seven). One wave gauge was positioned in front of each caisson to control the difference of the wave load (see Photo 5, Annex D), and two wave gauges were positioned behind the breakwater to record wave transmission by overtopping. In test phase B, only one wave gauge at a different position was used to measure wave transmission (see Figure 11). One further wave gauge was positioned beside the structure in order to get information on the wave height influenced by the slope but without the structure. The positions of the wave gauges are shown in Figure 11.

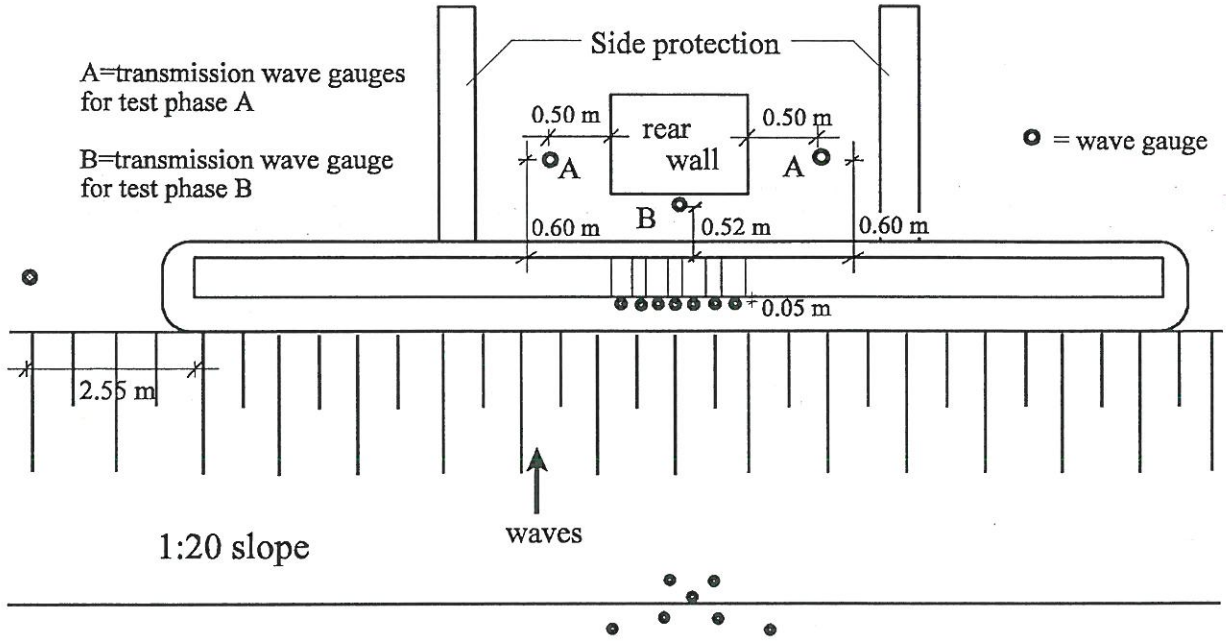

Figure 11: Position of wave gauges

The resistance type wave gauges were calibrated every morning by raising them 45 mm, acquiring a signal for 20 seconds at 100 Hz, then acquiring the zero level again for 20 seconds and calculating the calibration constants from the measured data. The calibration constants varied between 12 mm/V for the smaller wave gauges and 30 mm/V for the larger wave gauges.

The water depth was 0.50 m at the wave paddles, 0.30 m in front of the rubble mound foundation, and 0.20 m in front of the breakwater.

The complete model set-up is shown in Photo 6, Annex D.

3. Data acquisition

All transducers were connected to an amplifier which was connected to the acquisition computer. This computer used the acquisition programme DATS Acquisition Version V2.10 from Prosig Software Ltd.. The programme allowed to put in the sample rate and the acquisition length whereas the calibration constants have been inserted directly into the programme. In the project a continuous acquisition mode with a sample rate of 800 Hz for test configurations AA and AB and a sample rate of 400 Hz for test configurations BA and BB was used (except for the tests with non breaking waves

where a sample rate of 80 Hz was used). The high sample frequency was only needed for measuring pressures but in the acquisition system only one sample frequency for all channels could be chosen. The position of pressure and force transducers and wave gauges together with the amplifier and acquisition channels, amplification and filter values are given in Tables A1 to A4 in Annex A, respectively.

All data were first stored in a binary file (2 bytes per record) and later, after the acquisition was finished, the data were extracted to a DATS Dataset (*.dac-file, 4 bytes per record, real (4) format). All data were stored on CD-ROM in this *.dac-format. Table 1 gives an example of the structure of the *.dac file for a test, where two channels were recorded for 15 seconds at 10 Hz. A group of 512 bytes (128 pieces of information) is defined as a record. These records are used, because they can be read fast by software not reading every single value but the whole record. Every acquired channel is stored sequentially starting from the first channel. At the beginning of every channel there is one record with some basic information called header. The first value of the header is the number of acquired data (150 in the examples in table 1), the second is the acquisition rate (10 Hz in the example). Several of the remaining 126 values are zeros, some are description of the data (max. value, min. value etc.) and some

Table 1: Structure of *.dac-file

FILE Real(4)	Notes
150.0	HEADER 1st CHANNEL
10.0	
??	
??	
etc	
chan-1(1)	1st RECORD 1st CHANNEL
chan-1(2)	
chan-1(3)	
...	
chan-1(128)	
chan-1(129)	2nd RECORD 1st CHANNEL
chan-1(130)	
...	
chan-1(150)	
??	
??	
etc	
150.0	HEADER
10.0	
??	
??	
etc	
chan-2(1)	1st RECORD 2nd CHANNEL
chan-2(2)	
chan-2(3)	
...	
chan-2(128)	
chan-2(129)	2nd RECORD 2nd CHANNEL
chan-2(130)	
...	
chan-2(150)	
??	
??	
etc	
comments	extra RECORD
comments	extra RECORD

are not identified. At the end of all channels there is a description of the data that was unfortunately not updated during the tests.
In the example the 150 values are stored in two records, the first 128 values are stored in the first record and the remaining 22 in the second record, which is filled with 106 insignificant values.

4. Preliminary tests

4.1 Dry tests

The reason for the preliminary dry tests was to find out the response of the underlying rubble mound and the eigenfrequency of the system.
In the dry tests only the force transducers were connected and the basin was not filled with water. The force transducers were positioned as shown in Figure 12.

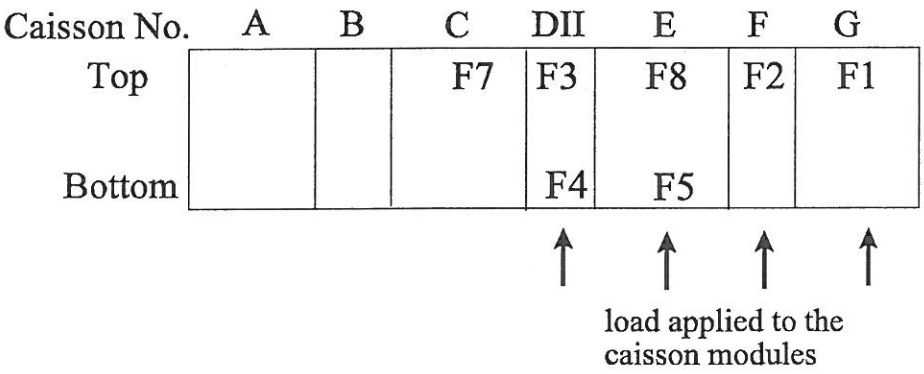

Figure 12: Position of force transducers for the preliminary tests

A 10 kg load was applied to one of the caisson modules horizontally, first as a static load and then as a dynamic load by hitting the 10 kg weight with a hammer. The force transducer signals were recorded for 50 seconds with an acquisition frequency of 800 Hz. To control the applied force, force transducer F6 was positioned at the front of the caisson, where the load was applied. For the first four tests, the force was applied on the top and the front of the module, then two other tests were performed, where the force was applied on the back and the bottom of the module (see Table 2).

Table 2: Preliminary dry tests

Test name	Force applied on module	Force transducers
dryst 01	F	upper
dryst 02	G	upper
dryst 03	E	upper and lower
dryst 04	DII	upper and lower
dryst 05	F	upper
dryst 06	DII	upper and lower

An preliminary analysis of the data resulted in an eigenfrequency of 40 Hz which was smaller than expected. Therefore the caisson stiffness was increased by filling them with more sand.

4.2 Measurements while filling the basin

The pressure transducers were positioned in the special centre module (configuration AA and AB). After the basin has been filled up to 40 cm water level, the pressure transducer signal has been recorded several times (at SWL of 40, 42, 45, 47.5 and 50 cm) to check the pressure transducers. They showed good results considering the fact that the pressure differences were close to the resolution.

4.3 Further preliminary investigations

Some test waves were generated to test the pressures and forces under impact conditions. These tests showed that the full measuring range of the pressure and force transducers was not used, so that the amplification factors were increased. The final amplification factors are given in Annex A.
Generating regular waves it was visually observed that the effect of diffraction from the ends of the breakwater is avoided by the lateral modules and the gravel.

5. Test parameters

5.1 Wave spectra and directional spreadings

All tests were performed with a modified type of the typical deep water JONSWAP wave spectrum. The modified JONSWAP spectrum is defined by the peak period T_P, significant wave height H_S and the peak enhancement factor γ. For most tests γ=3.3 was used, for some tests the JONSWAP-Spectrum with γ=1.0 was used that has less energy in the peak range. The two different spectra are shown in Figure 13.
The spectral density of the modified JONSWAP spectrum is:

$$S(f) = \frac{a\, H_S^2}{f^5}\, e^{-\left[1.25\left(\frac{f_p}{f}\right)^4\right]} \gamma^{e^{-\left[\frac{(f-f_p)^2}{2\,\sigma^2 f_p^2}\right]}} \quad [m^2 \cdot s] \tag{1}$$

$$\text{with:} \quad a = \frac{0.0624}{\left[0.230 + 0.0336\,\gamma - \frac{0.185}{1.9+\gamma}\right]} \quad [-] \tag{2}$$

$$f_p = \frac{1}{T_p} = \text{peak frequency} \tag{3}$$

γ=shape parameter, 1 to 7
σ=0.07 for $f \le f_P$
σ=0.09 for $f > f_P$

A directional spreading describes the distribution of wave energy around a mean direction. It can be described e.g. by a cosine function. In these experiments directional spreadings are described by

$$G(\theta) = N\cos^n(\theta-\theta_0), \text{ for } \theta_0-70° < \theta < \theta_0+70° \tag{4}$$

with: θ_0: mean wave direction
$G(\theta)$: spreading function
N: Normalizing factor

The directional spreading functions as used in the experiments are shown in Figure 14.

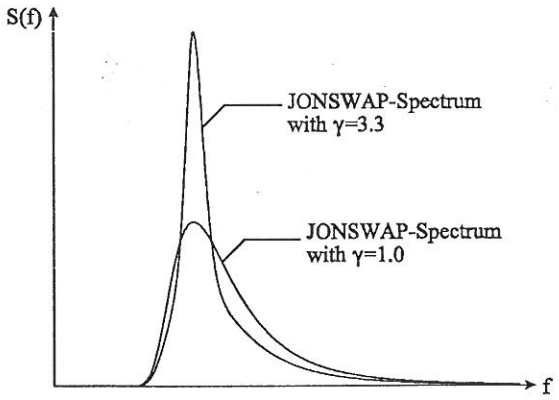

Figure 14: Wave spectra used in the experiment

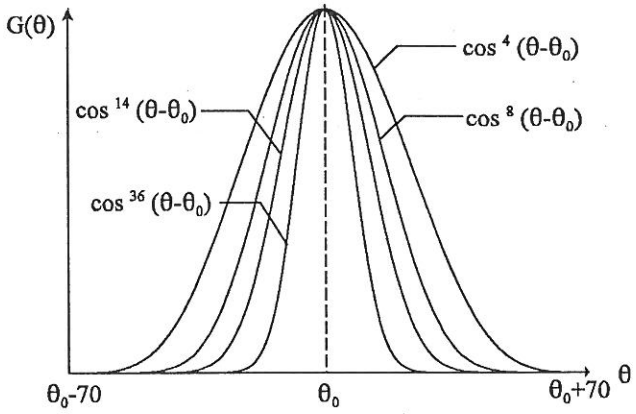

Figure 13: Directional spreading functions used in the experiment

A directional wave spectrum includes the direction in the concept of spectral density, so that the directional spectral density is described by $S(f,\theta)=S(f)G(\theta)$. An idealized directional spectrum is shown in Figure 15.

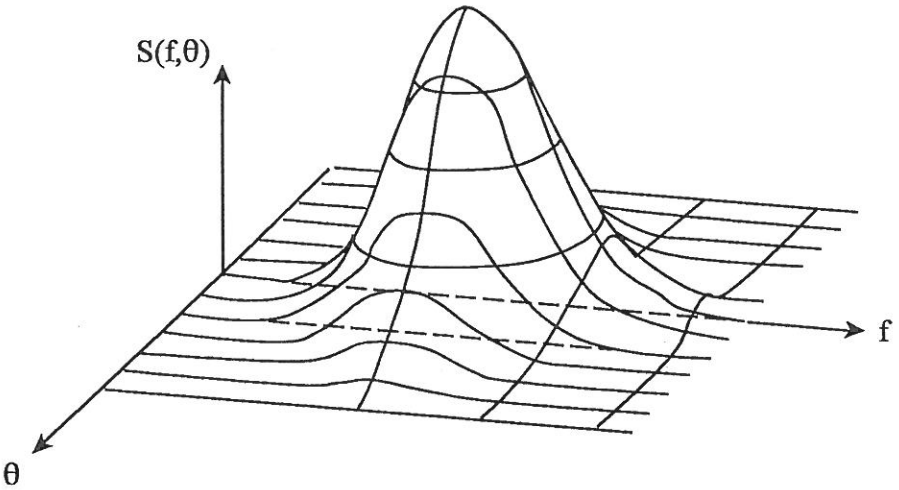

Figure 15: Directional wave spectrum

5.2 Wave generating system

The wave field was generated by 72 individual, electrically driven 0.5 m-wide piston wave paddle elements installed on one of the long sides of the basin (see Photo 7, Annex D).

The software HR WaveMaker (described in Beresford (1998)) was used to calculate the transfer functions from the input parameters to the wave generating signal, e.g. the necessary paddle movement for a certain wave height. For generating short-crested irregular waves with mean direction 0°, the software used a white noise random generator. The input parameters for the wave generating system were directional spreading and spectrum. For directional spreading the form $\cos^n(\theta)$ was used by input of the parameter n. Regarding the spectrum it could be chosen between JONSWAP, Pierson-Moskowitz and user-defined spectra. In this experiment the JONSWAP-spectrum was used with peak enhancement factor of either $\gamma=3.3$ or $\gamma=1.0$. Further input parameters for the spectrum were peak period T_P and significant wave height H_S. The user could give the initial sequence for the random generator, so that it was possible to repeat exactly the same paddle movements by giving the same input parameters and the same initial sequence. The wave paddles were used without absorption.

To generate oblique irregular short-crested waves, an input file was created that included the spectral energy density for 10 different directions and in each direction for 40 different frequencies. The frequencies were in the range from half the peak frequency to double the peak frequency, and the directions were between -40° to 40° from the mean direction. The spectral energy density was calculated so that it represented the input parameters such as spectrum, significant wave height and peak wave period. The software then calculated the required water surface elevation from the spectral energy density and from the water surface elevation the necessary paddle movements.

5.3 Wave heights and breaking frequency

After the preliminary test phase a revised test programme was developed defining the test phases AA, AB, BA and BB (see section 2.3). In this test programme, four different breaking frequencies (non-breaking, slightly breaking, heavy breaking, breaking and

broken waves) were fixed which were then connected to different wave heights. For the non-breaking waves an acquisition frequency of 80 Hz was used since no impacts were expected to occur. For the tests with breaking waves, an acquisition frequency of 800 Hz was used for test phase A and 400 Hz for test phase B. The number of waves for each test generally was 1000, all tests with a target breaking frequency of 2% were 2000 waves long in order to have a reasonable number of breakers for these tests (see Table 3).

Table 3: Characteristics of experiments

Test type	Significant wave height	Characteristics	Expected Breaking percentage	Acquisition rate [Hz]	No. of waves	Expected No. of breakers
W	6.5 or 8 cm	non breaking waves	0%	80	1000	0
X	10 cm	slightly breaking waves	2%	800 or 400	2000	40
Y	12 cm	heavy breaking waves	8%	800 or 400	1000	80
Z	14 cm	breaking and broken waves	>16%	800 or 400	1000	>160

The breaking percentages were related to target wave heights using visual observations. These wave heights were then used in the tests (given in Table 3). Besides the different wave heights, four different wave steepnesses, four different spreadings and two different spectral shapes were used. The default test were as follows, wave steepness of 4%, and directional spreading of 20°.

In the following Table 4 tests with bold letters (the letters are characteristic for wave heights as defined in Table 3) are primary tests with larger priority to be performed, the other tests are of secondary importance. All tests presented in the table have a mean

direction of 0°, some more tests with oblique mean wave direction have also been performed. A detailed table of all tests performed is given in Annex B.

Table 4: Test parameters

Configuration AA					
Spreading	$\cos^4\theta$=25°	$\cos^8\theta$=20°	$\cos^{14}\theta$=15°	$\cos^{36}\theta$=10°	$\cos^8\theta$=20°
Spectrum	Jonswap (γ=3.3)	Jonswap (γ=3.3)	Jonswap (γ=3.3)	Jonswap (γ=3.3)	Jonswap (γ=1.0)
Steepness					
5%		**WXYZ**			W YZ
4%	**WXYZ**	**WXYZ**	W Y	**WXYZ**	**WXYZ**
3%		**WXYZ**			W YZ
2%		**W Y**			
Configuration AB					
Spreading	$\cos^4\theta$=25°	$\cos^8\theta$=20°	$\cos^{14}\theta$=15°	$\cos^{36}\theta$=10°	$\cos^8\theta$=20°
Spectrum	Jonswap (γ=3.3)	Jonswap (γ=3.3)	Jonswap (γ=3.3)	Jonswap (γ=3.3)	Jonswap (γ=1.0)
Steepness					
5%		**W YZ**			W YZ
4%	**W YZ**	**W YZ**	W Y	**W YZ**	**W YZ**
3%		**W YZ**			W YZ
2%		**W Y**			

Configuration BA					
Spreading	$\cos^4\theta$=25°	$\cos^8\theta$=20°	$\cos^{14}\theta$=15°	$\cos^{36}\theta$=10°	$\cos^8\theta$=20
Spectrum	Jonswap (γ=3.3)	Jonswap (γ=3.3)	Jonswap (γ=3.3)	Jonswap (γ=3.3)	Jonswap (γ=1.0)
Steepness					
5%		**WXYZ**			W YZ
4%	**WXYZ**	**WXYZ**	**W Y**	**WXYZ**	**WXYZ**
3%		**WXYZ**			W YZ
2%		**W Y**			
Configuration BB					
Spreading	$\cos^4\theta$=25°	$\cos^8\theta$=20°	$\cos^{14}\theta$=15°	$\cos^{36}\theta$=10°	$\cos^8\theta$=20°
Spectrum	Jonswap (γ=3.3)	Jonswap (γ=3.3)	Jonswap (γ=3.3)	Jonswap (γ=3.3)	Jonswap (γ=1.0)
Steepness					
5%		**W YZ**			W YZ
4%	**W YZ**	**W YZ**	W Y	**W YZ**	**W YZ**
3%		**W YZ**			W YZ
2%		**W Y**			

To calculate the peak period from the wave height and the wave steepness, the following formula has been used:

$$T_{0p} = \sqrt{\frac{2\pi\ H_{0s}}{g\ s_p}} \qquad (5)$$

with: T_{0p}= peak period in deep water [s]
H_{0s}= significant wave height in deep water [m]
s_p= deep water wave steepness [-]
g = gravitational acceleration [m/s²]

It results from the deep water wave length:

$$L_0 = \frac{g\, T_{0p}^2}{2\,\pi} \tag{6}$$

with wave length $L_0 = \frac{H_{0s}}{s_p}$. (7)

6. Observations and in-situ analysis

6.1 Visual observations

During the tests, the breaking frequency and the overtopping have been visually observed. The occurrence frequency is divided as follows:

Table 5: Frequencies of breaking and overtopping

Qualitative judgement	Frequency
never	0
rare	< 1/100
frequent	about 1/10
normal	about 1/3

This classification was used for both, breaking and overtopping. The breaking has also been divided in type of breakers and location of breakers.

Table 6: Location and type of breaking waves

Location of breaking	Type of breaking
Breaking at wave paddles	spilling breaker and plunging breaker
Breaking on 1:20 slope	spilling breaker and plunging breaker
Breaking at the structure	flip through, plunging against wall, plunging before wall, roller hitting wall

The different types of breaking at the structure are principally shown in Figure 16.

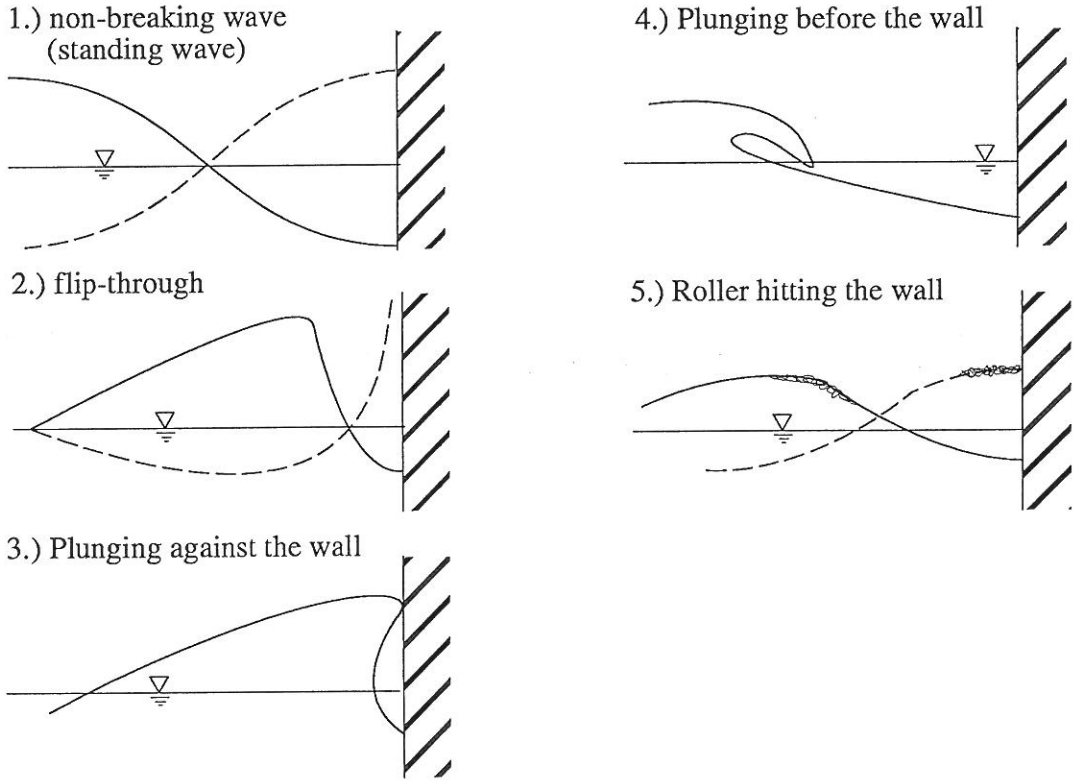

Figure 16: Different types of breaking at the breakwater

Spilling breakers were frequently observed at the wave paddles, their number was increasing with increasing wave height but almost no plunging breakers occured there. On the 1:20 slope, very few plunging breakers occured but only in tests with the highest wave height (H_s=14 cm). At the structure, the flip through breaker was predominant, all other breaker types only occured rarely. Overtopping was rarely observed in the tests

with non-breaking waves, increasing to normal frequency in the tests with higher wave heights.

A video camera has been installed in the basin showing the test section of the breakwater. Observations of the pictures taken by the video camera have been done in real time and many tests have been recorded on video tape (see Annex B).

The visual observations and other test parameters have been recorded on a form for each test. The forms for all tests are given in Annex F. Also, the collected data were quality checked frequently by looking at the time series. An example for a time series of pressure transducer, force transducer and wave gauges is given in Annex C.

6.2 Wave analysis

Short-crested waves are described by a directional wave spectrum which includes the wave energy distribution in both frequency and direction (see section 5.1).

There is no analytic solution available to calculate a directional wave spectrum from the water surface elevation so that estimation methods have to be used for wave analysis.

The main objective of the wave analysis in these experiments is to calculate the incoming deep water wave parameters from the array of wave gauges positioned at the toe of the 1:20 slope. Therefore, the wave field had to be split up in incident and reflected wave field.

The preliminary wave analysis has been performed with software developed by the Hydraulics and Coastal Engineering Laboratory of Aalborg University. Detailed information on the wave analysis can be found in the software manuals (AU, 1997 (1) and AU, 1997 (2)).

The wave analysis is divided into two steps. In the first step, spectral analysis is performed by calculating the auto-spectrum for each wave gauge of the wave gauge array and then the cross-spectra between all the wave gauges of the wave gauge array. The output of the spectral analysis is then used for the directional analysis, where two different estimation methods have been used:

(a) the Bayesian Directional Spectrum Estimation Method (BDM)

The method is based on Bayes theorem and is described in Hashimoto and Kobune (1988) and Helm-Petersen (1994). It has the advantage that there are no assumptions regarding the shape of the directional spreading function but it assumes a positive and smooth directional spreading function which can be expressed as a stepwise-constant function. The directional spreading function is discretized into a number of intervals and then iterations are performed from which the best estimate is chosen.
The output of the wave analysis using the BDM method were graphs of the total spectral density as function of frequency $S(f,\theta)$, the mean direction and the directional spreading of incident waves, the mean direction and the directional spreading of reflected waves and the reflection coefficients. Additionally, the significant wave height and the values of directional spreading for each frequency were given in a text file.

(b) the Maximum Likelihood Method (MLM)

In the directional wave analysis program using the MLM method three parameters were estimated: the mean incident direction, the directional spreading and the reflection coefficient. For using the Maximum Likelihoood Method, the distribution of the parameter to be estimated has to be known. Therefore, the shape of the directional spreading function was fixed. Details of the method can be found in Isobe (1990).
As a result of the wave analysis using the MLM method the significant wave height and the directional spreading, the main incident direction and the reflection coefficient as function of frequency were given in a text file.

During the wave analysis it was observed, that analysing the wave gauge array by the BDM method gave a high resolution for the full directional spectrum but with a low reliability. When the data from the wave gauge array were analysed by the MLM method the resolution was lower but the reliability was high. Spectra measured at the wave gauge at the side of the breakwater (wave gauge 14, see Figure 11) were calculated for comparison. Spectra measured in front of the caissons were also calculated which resulted in another value for the incident wave field which was then used for

comparison. Finally, the parameters from the MLM method were taken in most cases. Details of the wave analysis will be described in the technical report.

6.3 Comparison between force and integrated pressures

In the test configuration A pressures at the front of the breakwater and total forces at the rear side of the breakwater were measured. The integrated pressures should result in the wave induced horizontal force applied on the caisson. The force measured at the rear side of the structure should give a smaller value because of the influence of the mass of the structure, the friction of the rubble mound and other losses.
In order to compare the integrated pressures and measured forces a short test with the following wave parameters has been performed.

Table 7: Test parameters for test 98120202

Test name	98120202
test duration	20 sec (8 waves)
sample frequency	800 Hz
target wave height	12 cm
target wave period	1.55 sec
spectrum	JONSWAP (γ=3.3)
mean direction	0°
target directional spreading	25°

Some preliminary data analysis has been performed and is shown in the following figures. The pressures were integrated linearly. For the upper pressure transducers (the ones that were in air during the time of a wave trough) the hydrodynamic pressure was assumed to be the measured pressure minus the zero level of the pressure transducer (5%-fractile of minimum values) minus hydrostatic pressure. For the lower pressure transducers the hydrostatic pressure was assumed to be the mean value of the signal and the oscillating part was assumed to be the hydrodynamic pressure. In Fig.17 the

horizontal force components of the signals of the upper and lower force transducer have been added and are shown together with the results from the force computed from the seven integrated pressure signals at the front of the caisson. Fig. 18 shows the upper force transducer together with the sum of both force transducers. This shows the possibilities for further use of only the upper force transducers in test phase B.

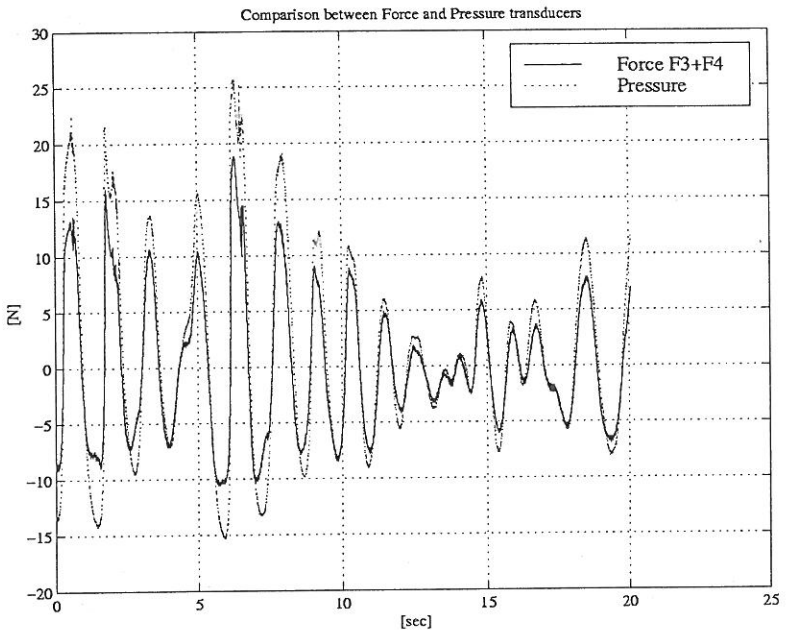

Figure 17: Sum of the two force signals and force from pressure signals for test 98120202

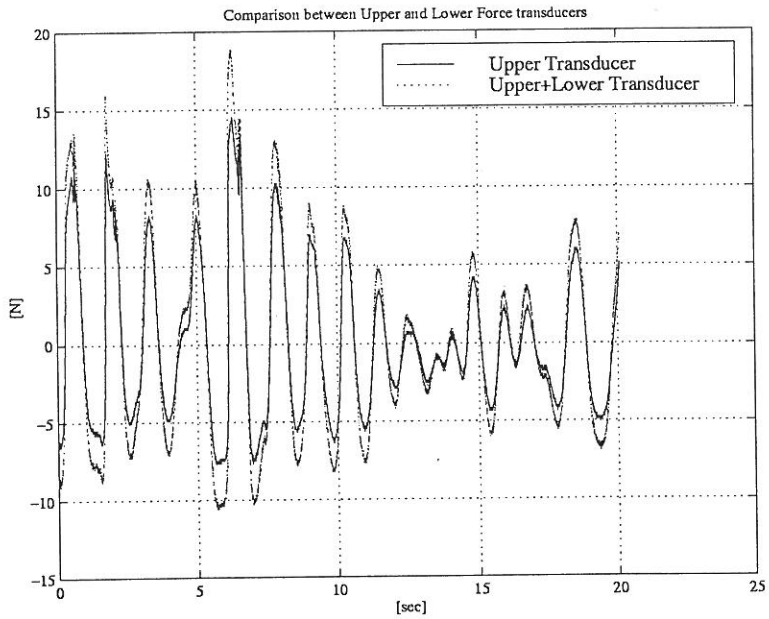

Figure 18: Comparison between upper force transducer and sum of both force transducers